JOURNAL OF CATALYSIS 141, 389–406 (1993)

Coke and Product Profiles Formed along the Catalyst Bed during *n*-Heptane Reforming

I. Nonsulfided Pt/Al_2O_3 and $Pt–Re/Al_2O_3$

C. A. QUERINI AND S. C. FUNG

Exxon Research and Engineering Company, Corporate Research Laboratories, Route 22 East, Annandale, New Jersey 08801

Received October 12, 1992; revised December 15, 1992

Deactivation of Pt/Al_2O_3 and $Pt–Re/Al_2O_3$ during *n*-heptane reforming was studied using a multi-outlet reactor, which allows determination of gas-phase composition profiles and coke profiles along the catalyst bed. Coke profiles strongly depend on catalyst type and pressure. At low pressure, 105 kPa, the coke content on the Pt catalyst increases along the bed and at 1225 kPa decreases. Between these pressure values, a maximum in the coke profile is observed. Similar changes in C_5 ring naphthene concentration profile with pressure are observed and a general correlation has been established between coke and C_5 naphthenes covering variations in time on-oil, pressure, and location of catalyst. Therefore, C_5 naphthenes appear as the dominant factor in the deactivation of these catalysts. The addition of Re to a Pt catalyst has a similar effect on the coke profile and on the C_5 naphthene profile of the Pt catalyst as increasing its operation pressure, i.e., shifting the maximum of coke and C_5 naphthene profile from bed outlet to inlet. Additionally, pressure at which coke is deposited affects TPO spectra. An increase in the total pressure of a Pt catalyst produces a TPO spectrum similar to that of Pt–Re. These results suggest that Re increases the hydrogen surface concentration on Pt–Re, and therefore, Re decreases the dehydrogenating capacity of this catalyst and increases its hydrogenating activity. The lower dehydrogenation activity of Pt–Re catalysts as compared with Pt catalysts results in forming less C_5 ring diolefins and, thus, Pt–Re catalysts exhibit lower coke make and better stability.

INTRODUCTION

Deactivation of naphtha reforming catalysts by coke deposition has been extensively studied during the last several years. Since the addition of Re to the bifunctional Pt/Al_2O_3 was first described in 1968 (*1*), the influence of additives on the behavior of the bifunctional Pt/Al_2O_3 catalyst has received considerable attention. The effect of Re and S (*2–6*), as well as the effect of other promoters, Ir (*6–10*), Sn (*11–15*), and Ge (*16–18*), on the activity and stability of Pt/Al_2O_3 has been reported. Coking is generally the main cause of deactivation during a catalyst cycle life (*19*). Factors that influence the quantity of coke that builds up on a given reforming catalyst include pressure, H_2/feed ratio, temperature, feed composition, and space velocity.

Although numerous studies have reported upon activity changes with space velocity (*20, 21*), the influence space velocity has on the stability of the reforming catalysts has received little attention. Wilde *et al.* (*22*) studied at atmospheric pressure the amount of coke deposited on both sulfided and unsulfided $Pt–Re/Al_2O_3$ using methylcyclopentane (MCP), n-hexane (nC_6), and *n*-heptane (nC_7) feedstocks at various space velocities. They observed that with all three feedstocks coke increased with decreasing space velocity. Similarly, Figoli *et al.* (*23*) studied the influence of the space velocity on the stability of Pt/Al_2O_3 using a full-range naphtha and obtained higher coke-make at lower space velocities.

The deactivation of Pt/Al_2O_3 is generally studied by adding promoters to the catalyst and by changing feed type and operating

0021-9517/93 $5.00

conditions. There are little published data comparing product and coke profiles along the catalyst bed. Recently, one such study by Fung *et al.* (*24*) reported product and coke profiles during nC_7 reforming over $Pt–Re/Al_2O_3$ in a multi-outlet reactor. This study shows that the coke distribution on the different catalytic sites changed along the catalyst bed and influenced the toluene concentration profile through the catalyst bed.

Coke profiles for several systems have been reported. Examples include: cumene cracking on zeolite catalyst (*25*), steam reforming of 1-methylnaphthalene on rhodium (*26*), isomerization of *n*-pentane on Pt/Al_2O_3 (*27*), and naphtha reforming on Pt/Al_2O_3 (*28*). Other examples are listed in Ref. (*29*). Coke profiles provide important mechanistic information. A series mechanism produces an increasing amount of coke throughout the bed, whereas a parallel mechanism yields a decreasing profile (*30, 31*). In more complicated reaction networks, coke deposits may result from a combination of pathways. If the main source of coke deposits is an intermediate compound, the coke profile will exhibit a maximum. On the other hand, in a consecutive system A $\rightarrow$ B $\rightarrow$ C, if coke comes from both A and C, there might be a minimum in the coke along the bed. Pore plugging due to very fast coking by a product may also introduce changes in the coke bed profile (*25*).

During regeneration of catalysts by coke burning, the coke profile may play an important role. Temperature increases, which can cause catalyst sintering, will be influenced by coke distribution in the catalyst bed (*25, 32*). Therefore, to optimize regeneration procedures, it is important to know the coke profile of a catalyst bed, especially when sintering is likely.

Complicated reaction patterns are displayed in catalytic reforming. During naphtha reforming, five-member ring naphthenes (C_5 naphthenes), notorious coke formers (*16, 35–42*) originally in the feed, display decreasing concentration profiles along the catalyst bed while heavier aromatics increase. Hydrogen partial pressure also changes along the reactor. These changes make it difficult to predict coke distribution along the catalyst bed. In the case of a pure hydrocarbon like nC_7, it is reasonable to assume that harmful heavy compounds build up along the reactor, while the concentration profile of C_5 naphthenes and H_2 depend on experimental conditions and catalysts. Although the positive and negative effect of each variable on catalyst coke-make is reasonably established, the inability to determine the relative magnitude of these variables in a given experiment hinders the prediction of the coke profile. Analyses of the coke profile and its relationship with the gas-phase composition is anticipated to provide information about the coking mechanism and the influence promoters and process conditions have on the behavior of Pt/Al_2O_3 catalysts.

In this paper, a multi-outlet reactor that allows product and coked-catalyst sampling along the bed was employed. The goal was to understand how coke profiles of Pt and Pt–Re catalysts are modified by operating conditions in the reforming of *n*-heptane. Coke profiles are correlated with the gas-phase product composition, in an attempt to establish which products are the most potent coke precursors. The influence of Re in such relationship is also discussed.

EXPERIMENTAL

Activity Tests

Figure 1 shows a diagram of the multi-outlet reactor. The liquid feed is mixed with H_2 in a vaporizer at 553 K before it is introduced in a downflow configuration into the preheat section of the reactor. The preheat section is packed with 0.16-cm ceramic spheres. This brings the feed temperature to the reaction temperature before it enters the catalyst bed. The reactor is fabricated from a 1.27-cm-o.d. stainless-steel tubing with an i.d. of 1.02 cm. It has four outlet ports along its wall where gas-phase samples

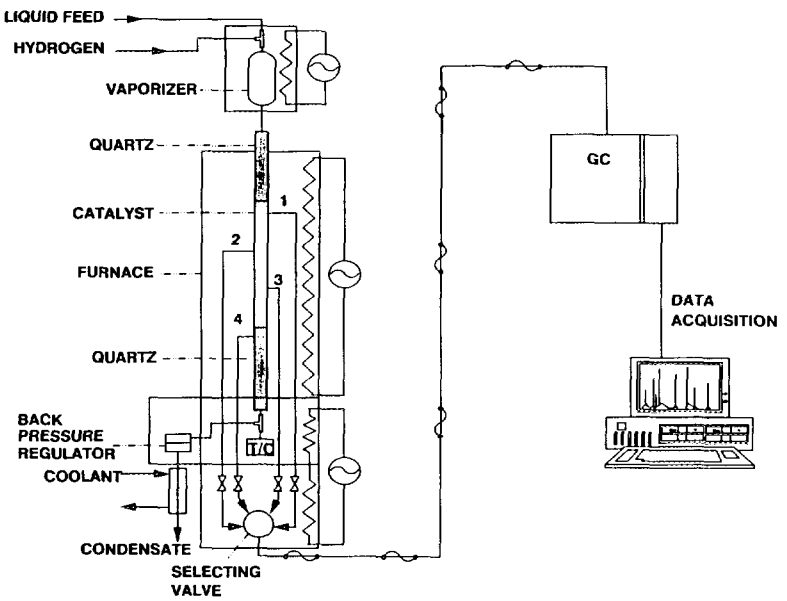

FIG. 1. Reactor scheme: 1, 2, 3, 4 indicate the outlets where a gas sample can be taken.

can be withdrawn. These four outlets are numbered 1, 2, 3, and 4 in Fig. 1. A three-zone furnace with independent temperature control provides the heat input to the reactor. This configuration makes it possible to achieve an isothermal wall profile along the length of the reactor where the catalysts are situated. During catalyst reduction, uniform temperature is also obtained at the center of the reactor along the entire length of the catalyst bed, about 33 cm, as is indicated by a multi-point thermocouple. The temperature controllers are programmed with a personal computer.

In a typical run, 20 g of catalyst are loaded above outlet 4. At outlet 4 the weight hourly space velocity is 2 w/w/h. The amount of catalyst placed above outlet 1 is 3.7% of the total charge. Therefore, the space velocity at outlet 1 is 54 w/w/h. The catalyst mass placed above outlet 2 is 40% of the total charge. This corresponds to a space velocity of 5 w/w/h. Similarly, the space velocity at outlet 3 is 2.9 since there is 70% catalyst above outlet 3. The catalyst is discharged in discrete sections without mixing so that the coke content of each section, matching those used to measure activity, can be analyzed. The amount of catalyst placed above outlet 1 is separated from the catalyst bed and is called section 1. The quantity of catalyst placed between outlet 1 and 2 is collected and is called section 2, and so on. A computer-controlled stream-selection valve automatically selects one of the outlets to be connected to the GC sample coil. A needle valve upstream of the stream-selection valve drops the pressure of the outlet stream to atmospheric pressure and controls its flow rate to the GC sample coil. The flow path of the sample stream is heat traced at 483–543 K to ensure that the total product is in the vapor phase. The sample stream is less than 5% of the total flow going through the catalyst bed and, therefore, it can be considered that there is little change in the space velocity due to the diversion of the sample stream.

After loading, the catalyst is reduced *in situ*, heating from room temperature to 788 K at 3 K/min, under 2000 cm^3/min of hydrogen. The catalyst is reduced at 788 K

for 8 h, then the reactor temperature is lowered to 643 K in 3 h before *n*-heptane is added to the reactor. Subsequently, the reactor temperature is increased over 3 h to the run temperature.

Experiments at 105, 350, 525, and 1225 kPa, and at 755 and 772 K were carried out. The weight overall hourly space velocity was 2 w/w/h and the hydrogen to hydrocarbon ratio was 3 in all the experiments. At the end of the specified run time, liquid feed to the reactor was stopped. The temperature of the reactor was lowered to 643 K over 3 h and maintained at this temperature for 5 h in hydrogen flowing at 430 cm^3/min. This procedure ensured the removal of adsorbed hydrocarbons so that they would not contribute to the temperature program oxidation (TPO) signal during the analysis of catalyst coke profiles. Following the 643 K hydrogen purge, the reactor was cooled to room temperature under flowing hydrogen. It should be emphasized that the catalyst was not presulfided and no sulfur was added to the *n*-heptane during the run.

On-oil time is counted from the moment the reactor attained the preselected reaction temperature. A 50-m capillary column coated with cross-linked methylsilicone gum provided a quantitative analysis of the components in the product. Data are collected and stored in a computer.

Coke Analyses

Coke was characterized by a highly sensitive temperature-programmed oxidation technique, using a modified Altamira TP unit (Model AMI-1). The modified unit converts CO_2 produced during coke oxidation to CH_4, using a Ru catalyst. The CH_4 is then continuously monitored with a flame ionization detector. This improves both sensitivity and resolution when compared with a thermal conductivity detector (TCD), which also requires a GC column to separate CO_2 from oxygen. Details of the technique have been reported (*33*). TPO analyses are performed using 1% O_2/He flowing at 60 cm^3/min through the sample while increasing temperature at a rate of 13 K/min from room temperature to 1043 K. Sample weight was generally 20 mg.

Catalysts

The monometallic catalyst contains 0.6 wt% Pt and 0.9 wt% Cl on Al_2O_3. The bimetallic Pt–Re/Al_2O_3 contained 0.3 wt% Pt, 0.3 wt% Re, and 0.9 wt% Cl. Both catalysts display a BET specific surface area of 200 m^2/g. They were used in the form of 0.16 cm diameter by 0.25- to 0.51-cm-length extrudate particles.

RESULTS

Reactor Temperature Profiles

Along the entire length of the reactor, the reactor wall is maintained at constant temperature by a three-zone furnace. During catalyst reduction, the temperature profile along the catalyst bed is flat, with less than 2 K variation as measured by a multi-point thermocouple in the center of the reactor. Due to the highly endothermic nature of the aromatization reaction, a steep temperature profile along the catalyst bed was observed when the nC_7 feed was introduced into the reactor. Figure 2 shows the temperature profile exhibited by Pt/Al_2O_3 as a function of time at 12, 19, 33, 43, 52, and 73% of catalyst bed. The reactor wall temperature was set at 772 K. At the start of the run, there was a 16 K drop in temperature at 12% of the catalyst bed. From this point on, the temperature drop along the catalyst bed became smaller and showed a value of zero beyond 73% of the catalyst bed. As the catalyst deactivated, the temperature drop in the catalyst bed decreased.

Product Profiles

Figure 3 shows the performance pattern of the Pt/Al_2O_3 catalyst along the catalyst bed in *n*-heptane reforming. Curve 1 indicates that the sample was taken from outlet 1. The equivalent space velocity at this point is 54 w/w/h since there is 3.7% catalyst mass above outlet 1. In a similar manner, curves 2, 3, and 4 represent samples taken at 40.4,

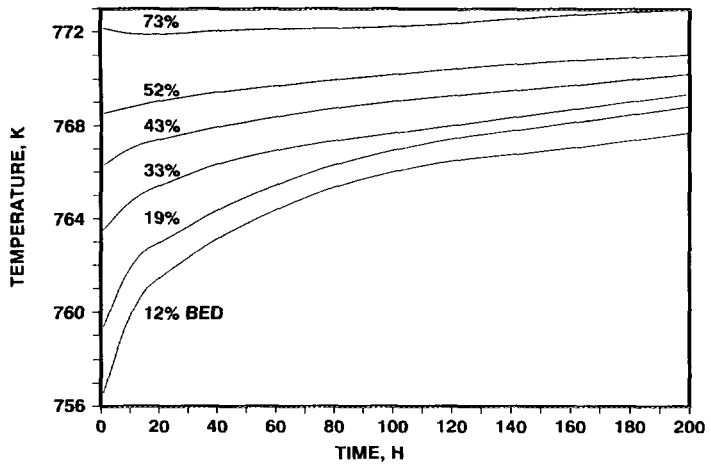

FIG. 2. Temperature profile along the bed as a function of time. Catalyst Pt/Al_2O_3. Temperature at reactor wall: 772 K.

70, and 100% of the catalyst bed at a corresponding space velocity of 5, 2.9, and 2 w/w/h, respectively.

With fresh catalysts, more than 40% of *n*-heptane is converted at outlet 1 after the feed passes through only 3.7% of the catalyst bed. At outlet 2, there is only 8 wt% of nC_7 left. The amount of nC_7 remaining at each of the outlets increases with on-oil time as the catalyst deactivates. At outlet 2, it reaches a value of 40 wt% after 200 h on-oil.

Concentration of toluene in the hydrocarbon mixture as a function of time at the four outlets is shown in Fig. 3B. After 200 h, the amount of toluene at outlet 4 is about one-third of the initial value (fresh catalyst). The majority of toluene is produced in the first 70% catalyst bed, since the concentration of nC_7 and *iso*-C_7, toluene precursors, in the last 30% catalyst bed are low.

Figure 3C shows the time dependence of 2-methylhexane (2MH) isomer at the four outlets. In each of them, the variations of 2MH concentration with time are different. At outlet 1 the amount of isomer decreases with time, at outlet 2 it goes through a maximum, and at outlet 3 and 4 it steadily increases with time.

With $Pt–Re/Al_2O_3$, similar nC_7 conversion and toluene and 2MH production profiles are obtained (see Fig. 3). The main difference is that after 40 h on-oil, nC_7 conversion over the bimetallic catalyst is essentially constant and the production of toluene and 2MH are also stable. Additionally, more light gases are produced by the bimetallic catalyst.

Figure 4 shows the amount of toluene as a function of the percentage of bed, for Pt and Pt–Re respectively. At time $t = 0$, the conversion to toluene is slightly higher over Pt than with Pt–Re, since the latter cracks more of the nC_7 feed to light gases. However, after a few hours on oil, the bimetallic Pt–Re catalyst remains more active than the monometallic Pt catalyst and maintains a constant activity after 60 h.

Slopes of the segments shown in Figs. 4A and 4B are proportional to the average reaction rate for toluene formation per unit of catalyst bed in a given section. In the case of Pt (Fig. 4A), as time increases the reaction rate in section 2 decreases faster than in section 3, and after 100 h they become similar. At longer times, it seems that the apparent reaction rate in section 2 becomes smaller than in section 3. However,

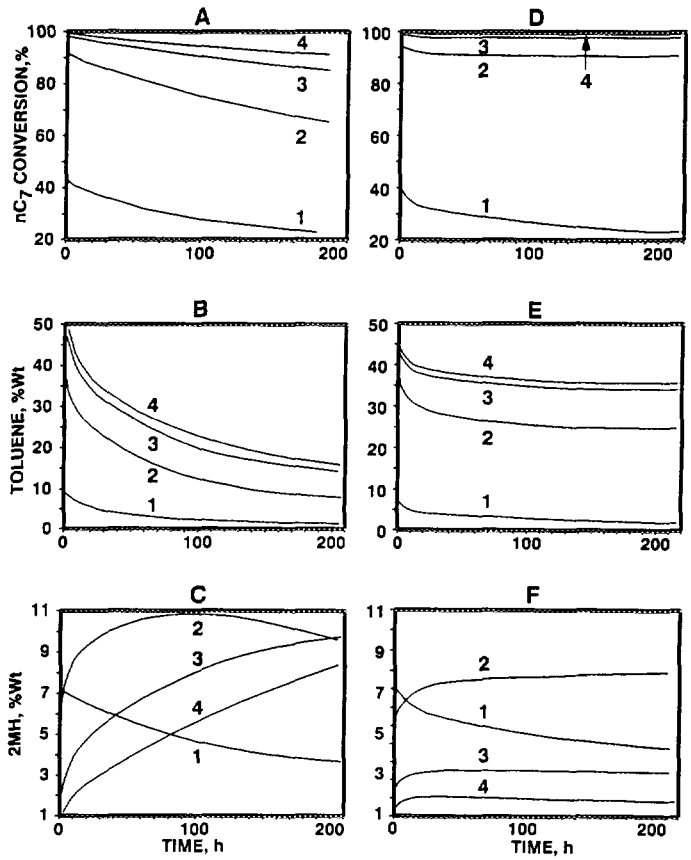

FIG. 3. Composition profiles for Pt: (A) nC_7, (B) toluene, (C) 2MH; and Pt–Re: (D) nC_7, (E) toluene, (F) 2MH. Labels: 1 : 3.7% bed; 2 : 40.4% bed; 3 : 70.7% bed; 4 : 100% bed. Feed, nC_7; temperature, 772 K; P = 525 kPa.

the highest toluene production rate remains in section 1 throughout the run. With Pt–Re, the maximum toluene production rate moves from section 1 to section 2 as the catalyst deactivates.

Because of the important role naphthenes (C_5 ring compounds) play in both dehydrocyclization and deactivation, compositional information about these compounds should be important. Figure 5 shows the variation of the total concentration of C_5 naphthenes methylcyclopentane, ethylcyclopentane (ECP), and dimethylcyclopentanes (DMCP) with time for Pt and Pt–Re at various working pressures.

At 772 K and 525 KPa, the initial amount of C_5 naphthenes at the four outlets is similar over both Pt and Pt–Re catalysts, with outlet 1 displaying the highest C_5 naphthene concentration. Interestingly, both catalysts show similar initial toluene levels at their corresponding outlets (Figs. 3B and 3E). With Pt–Re, there is a small increase in the C_5 naphthenes with time at the four outlets, and after 200 h, the maximum concentration of C_5 naphthenes is still located at outlet 1. In the case of Pt, after 15 h the maximum concentration of C_5 naphthenes is at outlet 2. Additionally, concentrations of C_5 naphthenes at outlets 2, 3, and 4 increase greatly with time on-oil to more than three times their initial values, although C_5 naphthenes

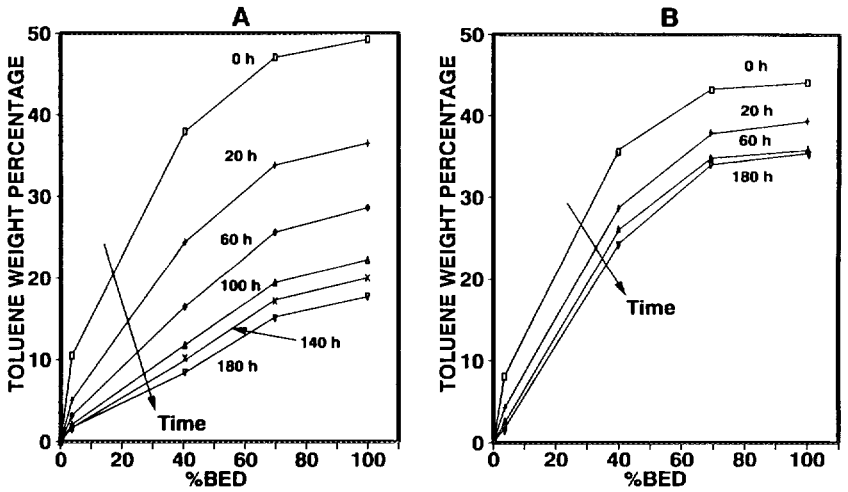

FIG. 4. Toluene concentration as a function of position in the bed. (A) Pt, (B) PtRe. Same conditions as in Fig. 3.

at outlet 1 does not deviate much from its initial value. After the initial on-oil period, large differences in the toluene levels at the four outlets are shown by the two catalysts.

Changing total pressure produces a significant change in the profile of C_5 naphthenes. When the operating pressure of Pt is increased to 1225 kPa, there is a systematic decrease in the total amount of C_5 naphthenes along the bed and the maximum always locates at outlet 1, similar to what happens with Pt–Re at 525 kPa. On the other hand, lowering the operating pressure of Pt–Re to 350 kPa results in C_5 naphthenes profiles similar to those of Pt at 525 kPa. The lower the pressure, the more the maximum concentration of these compounds shifts toward the end of the bed. At 105 kPa, the maximum is in section 4 (after some time on-oil).

The intermediate compounds C_7 olefins were observed at outlet 1 where the space velocity was high, 54 h^{-1}, corresponding to a contact time of 0.03 s. Under these conditions, the Pt and Pt–Re catalysts showed differences in their approach to equilibrium of heptane feed to heptene isomers. The partial pressures ratio of *cis*-3-heptene $* H_2/n$-heptane in section 1 (space velocity: 54 h^{-1}), at time zero, was 0.045 atm for Pt and 0.028 atm for Pt–Re, at 525 kPa and 772 K, and in the case of the *trans*-2-heptene $* H_2/n$-heptane ratio, its values were 0.052 for Pt and 0.032 for Pt–Re.

Figure 6 shows H_2 weight percentage and molar fraction for Pt and Pt–Re. The H_2 weight percentage increases along the bed from the 5.6% in the feed up to about 9% at outlet 4. There is no change in the H_2 weight percentage in the last 30% bed with Pt–Re. Initially the H_2 molar fraction displays a maximum centered within outlet 2 for both catalysts. This maximum disappears with time, and an overall decreasing profile is observed. This occurs quickly (within 15 h) with Pt–Re catalysts and does not show up until close to the end of the run with Pt catalysts.

Coke Profiles

The amounts of coke deposited (determined by TPO measurements) on the Pt and Pt–Re catalysts at various conditions are shown in Fig. 7. In these curves, the percentage values of coke for each section are assumed to be representative of the coke content in the middle of that section. With

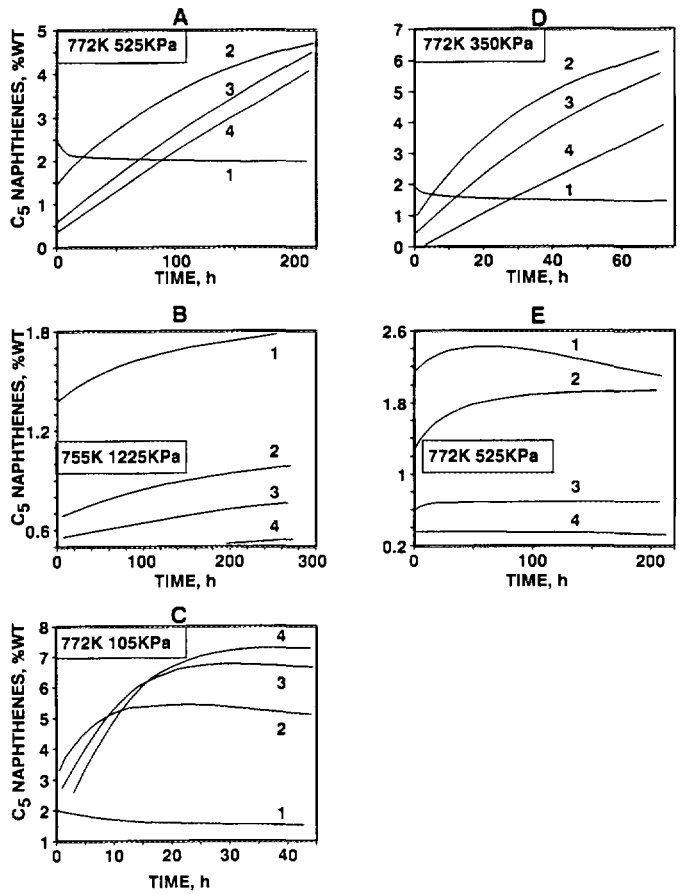

FIG. 5. C_5 naphthenes concentration profiles (MCP + ECP + DMCPs) for Pt: (A), (B), and (C). For Pt–Re: (D) and (E).

Pt, a maximum in the amount of coke along the catalyst bed is obtained at 525, 350, and 105 kPa, while a decreasing profile is observed at higher pressure (1225 kPa). The bimetallic produces a decreasing profile both at 525 and 1225 kPa, but a maximum is found at lower pressures, e.g., 350 kPa. In comparing Pt and Pt–Re in runs under similar conditions, the bimetallic catalyst is found to produce a lower amount of coke. Tables 1 and 2 summarize coke results for several runs over Pt and Pt–Re, respectively.

TPO Analyses

Temperature-programmed analyses of Pt and Pt–Re catalysts after 215 h on-oil at 525 kPa are shown in Fig. 8. Not only the amount of coke is different when comparing these two catalysts, but also the coke burning characteristics, as revealed by their TPO profiles. Pt shows two peaks well resolved at about 773 and 843 K. Pt–Re has only one peak well resolved at about 813 K, and another peak overlapping the main one at the lower temperature side of the peak. The relative size of these two peaks changes considerably with the sample position within the catalyst bed.

For comparison of coke characteristics, selected TPO spectra for Pt and Pt–Re removed from section 4 and coked under various conditions and time on-oil are presented in Fig. 9. In the case of the Pt catalyst, the

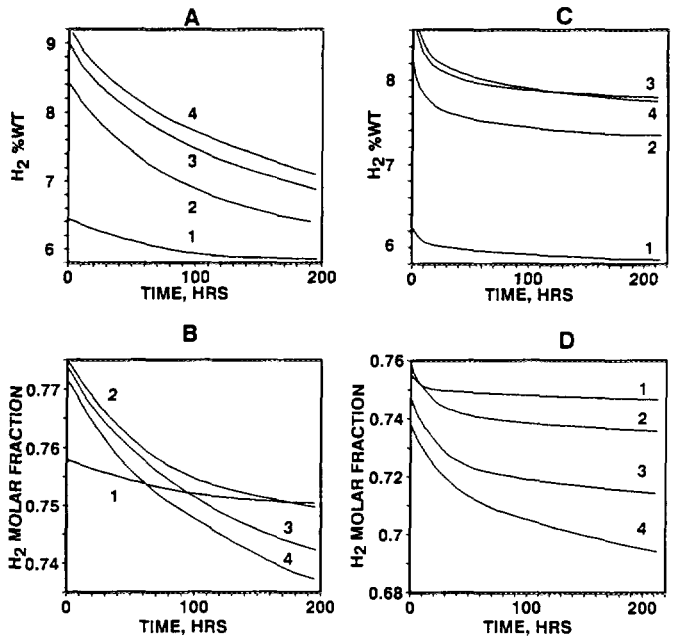

FIG. 6. Hydrogen concentration profiles for Pt: (A) weight percentage, (B) molar fraction. For Pt–Re: (C) weight percentage, (D) molar fraction. Same conditions as in Fig. 3.

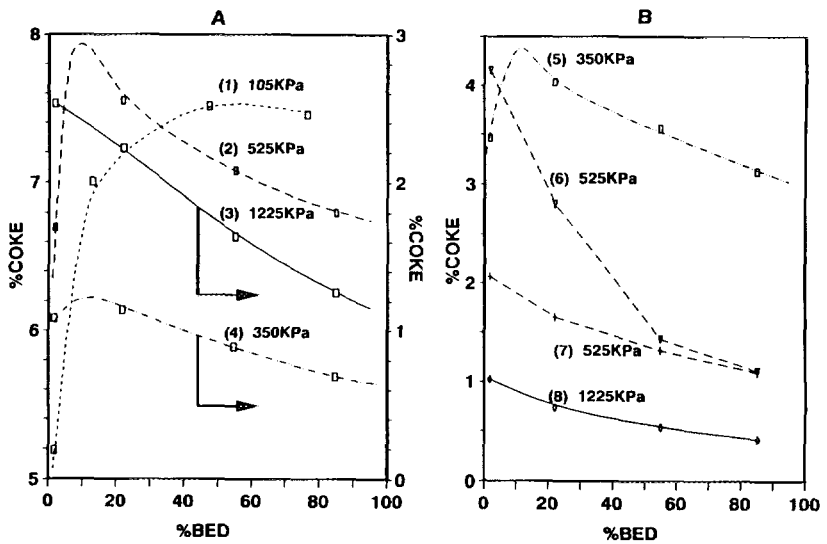

FIG. 7. Coke profiles along catalyst bed (A) Pt: (1) 772 K, 46 h; (2) 772 K, 251 h; (3) 755 K, 290 h; (4) 772 K, 2 h; (B) Pt–Re: (5) 772 K, 70 h; (6) 772 K, 213 h; (7) 755 K, 240 h; (8) 755 K, 123 h.

TABLE 1

Coke Content on Pt Catalysts

Temperature (K)	Pressure (kPa)	Time (h)	Bed (%):[a]	Coke (%) 1.9	22.1	55.1	84.9
772	350	2		1.08	1.14	0.89	0.69
772	525	24		2.11	2.13	1.74	1.36
772	525	72		3.54	3.57	2.89	2.56
772	525	120		4.89	5.02	—	—
772	525	215		6.70	7.55	7.08	6.80
755	1225	290		2.53	2.23	1.64	1.26

[a] The average coke level determined for each section is assumed to be representative of coke level at the middle of each section.

shoulder peaks at the left and right side of the main peak are better defined when the catalysts are operated at the high end of the pressure range and long on-oil time. At very short time on-oil, it is possible to distinguish the peak (below 673 K) that corresponds to coke on the metal particles (curve (8) in Fig. 9A and curve (5) in Fig. 9B). This peak becomes less distinct at longer time on-oil when coke level on the catalyst is increased.

DISCUSSION

Coke Profiles

Major differences in the coke profiles are obtained when comparing Pt with Pt–Re, or for a given catalyst with changes in reaction pressure. Several factors play a role in the amount of coke deposited on a catalyst during hydrocarbon reforming. These are included in Table 3 and are briefly discussed. Coking is the main cause of deactivation during a normal on-oil operation (*19*). Several factors influence the amount of coke build-up on a given reforming catalyst. These include pressure, H_2/feed ratio, temperature, feed composition, and space velocity. It has been found that the higher the total pressures and/or the H_2/feed ratios, the lower the amount of coke deposited on the catalyst (*8, 19, 23, 34–36*) because lower amounts of olefins are produced under these conditions. For a given hydrocarbon, the amounts of diolefins being produced depend on the hydrocarbon and hydrogen partial pressures. Coke formation occurs with an apparent activation energy between 20 and 40 kcal/mol (*19*) and, therefore, an increase in the reaction temperature enhances coking and the deactivation of the catalyst (*19, 23, 34, 37*). The influence of feed composition and molecular structure on the amount of coke deposit has been reported in several articles (*16, 35–42*). Experiments with pure hydrocarbons (*16, 35–37, 40*) show that C_5 naphthenes, as well as high-molecular-weight compounds, are very effective coke precursors. When naphthas are used as feed, it is found that lighter cuts (mean boiling point less than 383 K) produce more deactivation than intermediate boiling range naphthas (mean boiling point around 383 K), supposedly because of a higher concentration of C_5 naphthenes. On the other hand, heavier cuts also produce more deactivation because of high concentrations of C_9- compounds present in these feeds (*41, 42*). Results similar to those obtained with pure hydrocarbons are obtained when using a low-coke-make naphtha doped with 10 wt% hydrocarbons (*39*).

In the present study, the variation of temperature and C_{10}+ fraction along the catalyst bed is shown in Table 3 and according to the above discussion would make a coke profile increasing from bed inlet to outlet. As was previously discussed, the lower the

TABLE 2

Coke Content on Pt–Re Catalysts

Temperature (K)	Pressure (kPa)	Time (h)	Bed (%):	Coke (%) 1.9	22.1	55.1	84.9
772	525	2		0.31	0.34	0.33	0.30
772	525	24		0.99	0.95	0.69	0.58
772	525	32		1.19	1.08	0.83	0.68
772	525	72		2.35	2.18	1.21	0.84
772	525	91		2.43	1.92	1.09	0.97
772	525	120		2.87	2.57	1.53	1.10
772	525	213		4.16	2.81	1.44	1.12
755	525	330		2.06	1.48	1.18	1.05
755	525	240		2.07	1.66	1.32	1.10
755	1225	24		0.56	0.54	0.46	0.40
755	1225	123		1.03	0.74	0.54	0.42

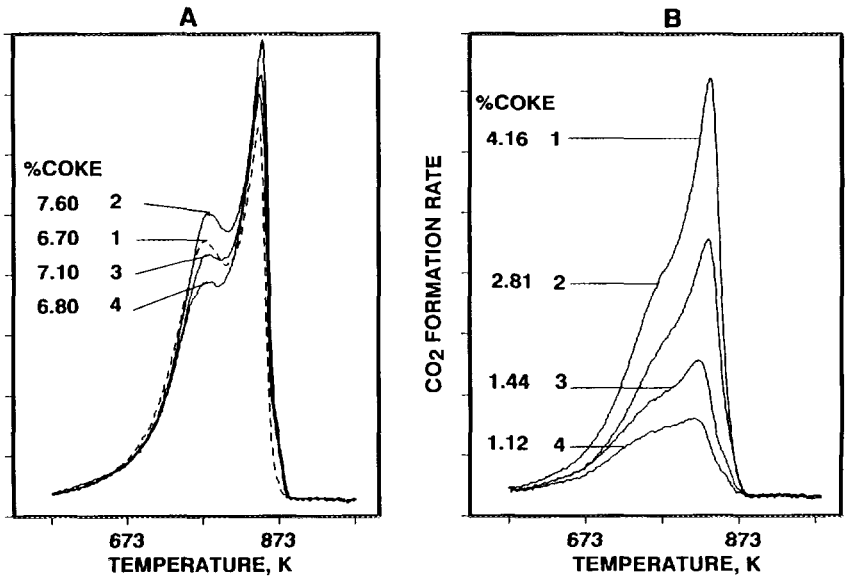

FIG. 8. TPO of coked catalysts (A) Pt, (B) Pt–Re. Heating rate, 13 K/min; carrier gas, 1% O_2/He. Time on-oil, 215 h; coking conditions, same as in Fig. 3.

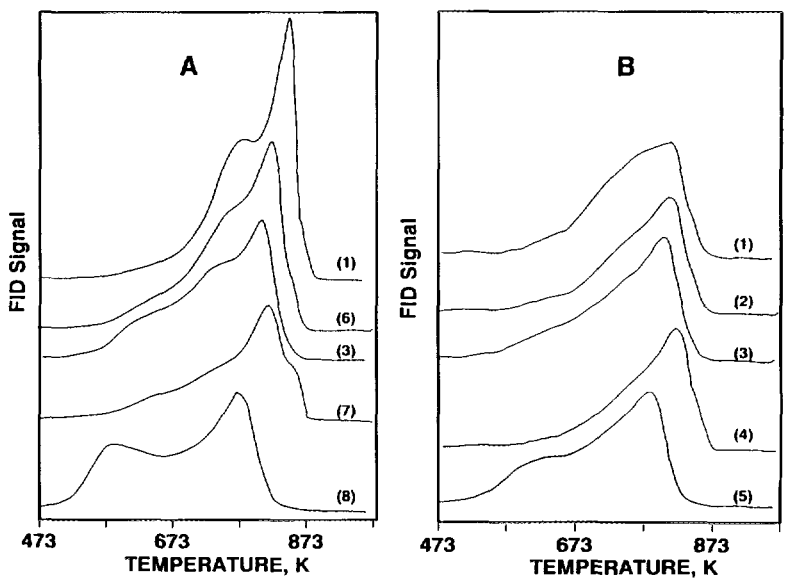

FIG. 9. TPO of selected samples (from Section 4). (A) Pt, (B) Pt–Re. (1) 525 kPa, 772 K, 215 h; (2) 525 kPa, 772 K, 120 h; (3) 525 kPa, 772 K, 24 h; (4) 525 kPa, 755 K, 330 h; (5) 525 kPa, 772 K, 2 h; (6) 525 kPa, 772 K, 72 h; (7) 1225 kPa, 755 K, 290 h; (8) 350 kPa, 772 K, 2.5 h.

TABLE 3

Factors that Affect Coke Deposition and Their Variations along the Bed, during *n*-Heptane Reforming

Factor	Change along the bed	Coke along the bed should
Temperature	Increase	Increase
H_2 partial pressure	(i) Decrease (ii) Maximum	(i) Increase (ii) Minimum
C_{10+} fraction	Increase	Increase
C_5 naphthenes	(i) Decrease (ii) Maximum	(i) Decrease (ii) Maximum

hydrogen partial pressure, the faster the catalyst deactivates (*8, 19, 23, 34–36*). Therefore, the existence of either a maximum or a decreasing H_2 partial pressure in the catalyst bed should produce a minimum or an increasing coke profile. These two coke profiles were not observed experimentally. It should be pointed out that the changes in the partial pressure of H_2 are rather small, with a maximum variation of 8% along the bed.

The C_5 naphthenes have a decreasing concentration profile from outlet 1 to outlet 4 or exhibit a maximum depending upon the catalyst and the total pressure (Fig. 5). With Pt–Re at 525 kPa and Pt at 1225 kPa, their C_5 naphthenes concentrations decrease from outlet 1 to outlet 4 (Fig. 5). Their coke profiles also decrease from section 1 to section 4 (Fig. 7). With Pt at 525 kPa and Pt–Re at 350 kPa, the C_5 naphthene concentration shows a maximum at outlet 2, and the coke profiles in both cases also show a maximum located in section 2. At lower pressures, such as 105 kPa, the Pt catalyst shows a maximum of C_5 naphthenes in section 3 or 4, the same section where coke-make is maximum. This suggests the existence of a correlation between C_5 naphthene concentration and the coke-make along the catalyst bed for both Pt and Pt–Re. Indeed Fig. 10 shows a direct correlation between the amount of coke deposited in each catalyst section after 215 h on-oil and the time-average C_5 naphthene concentration at each outlet. Both catalysts show a linear relationship between coke and C_5 naphthene concentration, but for a certain amount of C_5 naphthenes, Pt produces more coke than Pt–Re. For example, for a time-average C_5 naphthene concentration of 2 wt%, the coke-make on Pt is 6.6% and on Pt–Re is 1.8%.

These results suggest that C_5 naphthenes concentration is the dominant variable in the coking and deactivation of reforming catalysts during nC_7 aromatization.

The concentration of C_5 naphthenes in the reactor inlet is zero when pure nC_7 is used as feed. Therefore, in all runs, there is a maximum in the concentration of C_5 naphthenes along the bed. According to the results showed in Fig. 5 at 525 kPa, 772 K, and WHSV = 2, with Pt–Re this maximum is located at the very top of the catalyst bed, before 3.7% bed. When Pt is the catalyst, after 10 h on-oil, the maximum in C_5 naphthene concentration is located between 3.7 and 40% of bed, moving downstream as time increases. It appears that a maximum in C_5 naphthenes always exists and, therefore, a maximum in coke should always be found. In the case of Pt–Re, the maximum is so close to the top of the reactor that it is not possible to divide the bed in fractions small enough to locate the coke maximum.

Both the Pt and Pt–Re exhibit the same qualitative behavior, but differ quantitatively. The influence of Re is not to reduce the initial amount of C_5 naphthenes, but to slow down their conversion to coke. Figure 5A and 5E show that initially the amount of C_5 naphthenes at each of their four corresponding outlets is roughly the same for Pt and Pt–Re at 525 kPa and 772 K. This indicates that there is no preferential destruction of these compounds by Pt–Re as was suggested earlier (*43*), although Pt–Re exhibits higher hydrogenolysis activity than Pt. This observation agrees with the conclusion of Burch and Mitchell (*11*), who studied cyclopentadiene reactions on Pt, Pt–Re, and Pt–Sn, and suggested that the role of Re was not to open the C_5 ring, but to in-

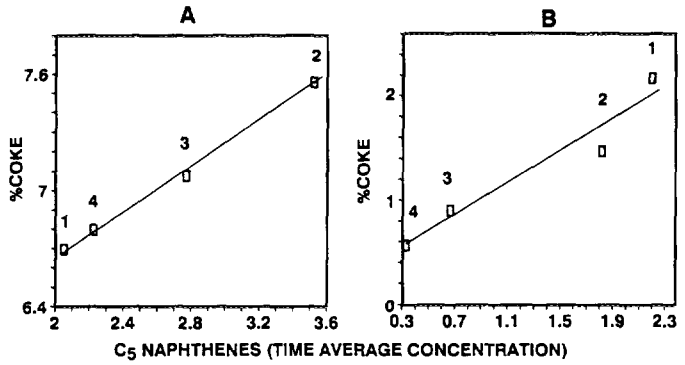

FIG. 10. Percentage coke vs time average of C_5 naphthenes concentration. (A) Pt; (B) Pt–Re. Same conditions and time on-oil as in Fig. 3. Numbers refer to the section from which the sample was taken.

crease the hydrogenating capacity of the catalyst. Other authors also related the improvement in the stability of bimetallic catalysts by considering their lower dehydrogenating capacity (*3*, *36*). The lower dehydrogenation activity of a bimetallic catalyst minimizes the formation of C_5 ring diolefins, which leads to coke formation on the alumina support acid sites through Diels–Alder condensation and polymerization reactions (*36*, *44*). This agrees with the smaller ratios of partial pressures of (*cis*-3-heptene $* H_2/n$-heptane) and (*trans*-2-heptene $* H_2/n$-heptane) obtained with the Pt–Re catalyst as compared to those of the Pt catalyst, indicating a lower dehydrogenating activity of the bimetallic catalyst. The lower dehydrogenating and higher hydrogenating activity could be due to a higher H_2 surface concentration and are discussed in detail later.

The steady increase in the C_5 naphthenes concentration observed at outlets 2, 3, and 4 in Fig. 5A as the Pt catalyst deactivates (525 kPa) corresponds to the behavior of an intermediate in a consecutive reaction scheme $A \xrightarrow{k_1} B \xrightarrow{k_2} C$. The concentration of B as a function of contact time is shown in Fig. 11. When a catalyst deactivates, the effect is similar to that of reducing the amount of catalyst and, therefore, to decreasing the contact time. As a consequence, the point that represent the concentration of B in a given location in the catalyst bed moves from right to left along the curve in Fig. 11. If the initial contact time is on the right of the maximum (low space velocity or away from the top portion of the catalyst bed), the deactivation should produce an increase in the concentration of B (points 2, 3, and 4 in Fig. 11 move to the left), and eventually the concentration of B goes through the maximum and then decreases. This effect is enhanced if k_2 decreases more than k_1, i.e., higher coking on acid sites than on metal. The acid sites are essential in maintaining low C_5 naphthenes concentration through ring expansion to the C_6 ring

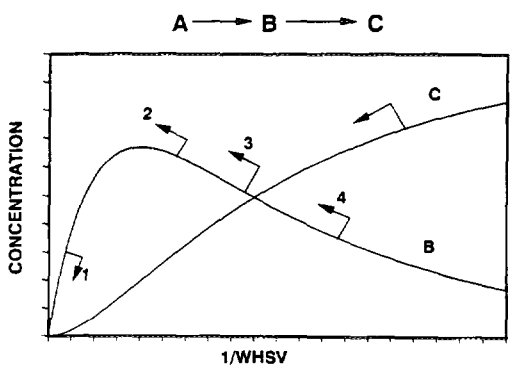

FIG. 11. Plot of concentration vs residence time (1/WHSV) for compounds B and C in the system: $A \rightarrow B \rightarrow C$.

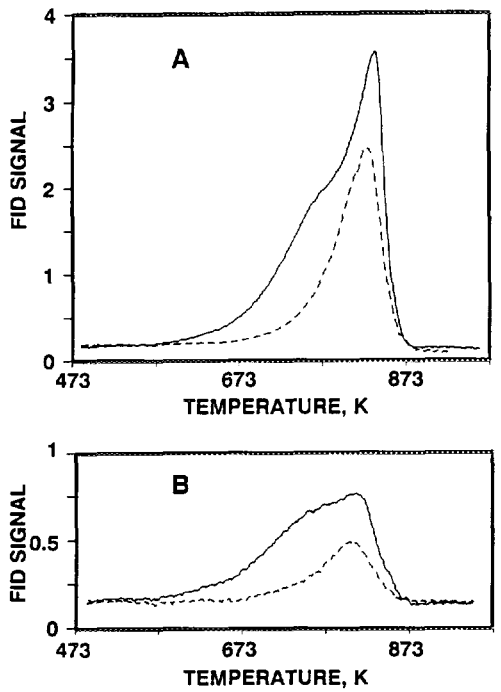

FIG. 12. TPO of Pt–Re catalyst. Coking conditions, same as in Fig. 3. (A) Sample from top of the reactor, (B) sample from bottom of the reactor. (—) TPO of discharged samples; (---) TPO after partial regeneration, heating from room temperature to 723 K, holding at this temperature for 15 min.

and its subsequent essentially irreversible dehydrogenation on the metal sites to stable aromatics. When the initial contact time is on the left of the maximum, the deactivation of the catalyst produces a decrease in the amount of the intermediate, as shown by point 1 in Fig. 12 and curve 1 in Fig. 5A.

Pressure affects both catalysts in their coke distribution along the bed. A decrease in the total pressure (which implies a decrease in H_2 partial pressure) shifts the maximum of the coke profile downstream, e.g., at 525 kPa, and the maximum could not be detected for Pt–Re (i.e., it is located upstream of the 3.7% bed), while at 350 kPa, the maximum is between 3.7 and 40% bed. Pt/Al_2O_3 produces a decreasing coke profile at 1225 kPa, and shows a maximum at lower pressures (525, 350, 105 kPa). At 105 kPa, the maximum is near the bottom of the catalyst bed. This means that working at low enough pressures, it is possible to obtain an increasing coke profile along the catalyst bed, as has been reported in (*22*). Coke profile and toluene stability obtained with Pt at 1225 kPa is similar to the one obtained with Pt–Re at 525 kPa. Therefore, the monometallic catalyst behaves similar to the bimetallic one with regard to coke profile and catalyst deactivation, when the former are operated at higher pressures.

The significant differences in the amount of coke along the bed indicate that studies of deactivation of reforming catalysts using low space velocities would give the average amount of coke when the coke analysis is performed on a portion of a well-mixed discharged catalyst. Furthermore, any model dealing with catalyst deactivation should take this fact into consideration to capture the effect of nonuniform catalyst deactivation.

Isomerization

The C_7 isomer concentration profiles along the bed and their change with time clearly shows that these compounds are intermediates in the nC_7 reforming network. The concentration of 2MH shows a continuous decrease at outlet 1, a maximum at outlet 2, and a continuous increase at outlet 3 and 4 with time on-oil (Fig. 3B). This unusual behavior is expected based on Fig. 11 by moving points 1, 2, 3, and 4 to the left at increasing catalyst deactivation. The four points in Fig. 11 can be viewed as the contact time experienced by the catalyst situated upstream of outlet 1, 2, 3, and 4, respectively.

Similar behavior was observed for other C_7 isomers, as well as C_6 and C_5 isomers. Nevertheless, *iso*-C_4 follows the behavior of a final product, i.e., with an increase in its concentration along the bed and a decrease at each position with time. This suggests that there is no significant destruction of *iso*-C_4 due to cracking.

Hydrogen Profiles

Although there is net production of H_2 along the bed, as indicated by the increase in its weight percentage, the concentration expressed as molar fraction decreases with Pt–Re (after 15 h) and shows a maximum with Pt (Fig. 6). This means that in the case of Pt–Re, dehydrocyclization and cracking along the catalyst bed result in a net increase in hydrogen (moles) which is less than three times the net increase in hydrocarbons (moles) since at the inlet the hydrogen to feed ratio is 3/1. In less than 20 h on-oil, the molar fraction of hydrogen in all four outlets is below the inlet value of 0.75. The Pt catalyst shows lower cracking activity and, therefore, the production of hydrogen along the catalyst bed leads to increasing hydrogen molar fraction until at a point, where the dehydrocyclization rate decreases more than the cracking rate, the hydrogen molar fraction decreases. As the catalyst deactivates, the dehydrocyclization rate falls below that of the cracking rate to such an extent that it fails to maintain the hydrogen molar fraction at 0.75 at outlet 3 and 4. The high hydrocracking activities in these two catalysts result from a lack of sulfur on the catalysts and in the feed. Pt–Re exhibits a higher hydrocracking rate than Pt and, therefore, a higher H_2 molar fraction is obtained with Pt along the entire bed.

Aromatization

With a fresh catalyst, one expects that the average toluene production rate in section 1 (3.7% bed) is higher than that in section 2 (from 3.7 to 40.4%) and decreases even further from section 2 to section 4 since the average feed concentration drops sharply from section 1 to section 4. This was observed with both Pt and Pt–Re catalysts. At increasing extent of catalyst deactivation, the mono- and bimetallic catalysts behave differently. With Pt–Re, the first section of the catalyst becomes less active in toluene production than the catalyst in the second section after 60 h on oil. In the case of Pt, the second section becomes less active than the third after 140 h. These changes of toluene production rates as a function of time can be interpreted taking into account the differing amounts of coke deposited on these two catalysts in each section.

In the case of Pt–Re, section 1 has the highest amount of coke and exhibits the highest deactivation. Catalyst activity loss surpasses the feed concentration advantage and results in moving the maximum toluene production rate into section 2 after 60 h on-oil. In the case of Pt, a different situation arises. The highest coke level is located in section 2. Therefore, the maximum toluene production rate remains in section 1 throughout the run. However, the toluene production rate in section 2 is lower than that in section 3 at 140 h on-oil since section 2 shows the highest coke level. Therefore, the difference in the movement of the maximum toluene production rate in the catalyst beds, as the mono- and bimetallic catalysts deactivates, is the result of different coke profiles exhibited by these catalysts.

TPO Analyses

The TPO profiles (Figs. 8 and 9) show that the changes in pressure and time on-oil produce modifications in the relative amount of various types of coke. High operation pressure greatly decreases the coke-make on Pt catalysts when they are compared at the same run length (Table 1). When Pt catalysts being operated at high and low pressures are compared at about the same coke level, the peak temperature in the TPO spectrum of coke deposited at 1225 kPa on the Pt catalyst (curve (7), Fig. 9A, 1.26 wt% C after 290 h on-oil) shifts to a higher temperature when it is compared to coke deposited at 525 kPa (curve (3), Fig. 9A, 1.36 wt% C after 24 h on-oil). Additionally, the catalyst coked at higher pressure shows less coke being burned below 673 K than the catalyst coked at lower pressure. Similar effects were reported by Barbier *et al.* (*34*) in their Pt/Al_2O_3 catalyst deactivation study using cyclopentane. Additionally, they re-

ported that the coke formed at high pressure showed a lower H/C ratio than coked formed at low pressure. This is partly due to a lower amount of coke forming on the metal (coke on metal has higher H/C ratio than coke on support) but is predominantly due to more dehydrogenated coke forming on the support at higher pressure, as indicated by a higher peak temperature in its TPO spectrum. Both the lower H/C ratio and the higher peak temperature suggest a higher degree of graphitization of the coke in the high-pressure run because a substantially longer time is provided for the graphitization process due to its longer run length.

The coke deposited on the Pt catalyst at 1225 kPa (curve (7), Fig. 9A) shows a TPO spectrum similar to coke deposited on Pt–Re at 525 kPa (curve (4), Fig. 9B). These two catalysts have about the same coke level, 1.26 and 1.05 wt%, and run length, 290 and 330 h, respectively. This suggests that coke characteristics, like degree of polymerization (H/C ratio), location of coke, etc., are strongly affected by H_2 partial pressure and that Pt requires higher pressures to produce a coke similar to that of Pt–Re. It appears that the presence of Re increases the surface concentration of hydrogen in the Pt–Re catalyst. This higher H_2 surface fugacity may be responsible for the lower dehydrogenating activity of the bimetallic catalyst and as a consequence, it minimizes the formation of C_5 ring diolefins and lowers the coke-make. It has been reported that addition of metals like Ga and Zn on H-ZSM5 greatly decrease the hydrogen surface fugacities and, therefore, modify the selectivity and activity of the catalyst for alkane reactions (*45*, *46*). Therefore, Re may act in a similar manner, although in an opposite way, as Ga or Zn in H-ZSM5.

At very short time on-oil, it is possible to distinguish the peak that corresponds to coke on metal (curves (8), Fig. 9A; curve (5), Fig. 9B). At higher coke contents, this peak is buried by the whole envelope, because coke on the metal builds up at the beginning of the experiment, reaching a pseudo-steady state (*6*) at a relatively low level.

It is interesting to compare the TPO spectrum of the Pt–Re taken from the top of the reactor with a sample taken from the bottom (Fig. 8). Obviously both samples were run under the same conditions, but exposed to different gas-phase composition. The top sample was exposed mainly to the highest concentration of C_5 naphthenes and the lowest of C_{10^+} fraction. The opposite was experienced by the bottom sample. It seems that the fraction of coke burned below 773 K, in the section 1 sample is smaller than the section 4 sample and can be determined experimentally. A partial coke burn of the above two samples was performed in a TPO experiment by limiting its maximum temperature to 723 K and holding it at this temperature for 15 min before cooling to room temperature in helium. The quantity of coke remaining after the first TPO was determined by a second TPO carried out to 1043 K (dash curves in Fig. 12). The percentage of coke removed from the section 1 and section 2 samples by the first TPO (low temperature) is 50 and 63, respectively. These results indicate that the gas-phase composition has an influence on the distribution of coke on the catalyst surface. The heterogeneous coke distribution along the bed implies that different proportions of coke will be removed during low-temperature (e.g., below 773 K) regeneration of the catalyst bed.

CONCLUSIONS

The addition of Re to Pt significantly affects its coke and product profiles along the catalyst bed. Re addition has a similar effect as increasing the pressure; i.e., it shifts the maximum in the coke profile toward the inlet of the bed. At low pressure, 105 kPa, the coke content on the Pt catalyst increases along the bed and at 1225 kPa, the coke content on the Pt catalyst decreases from inlet to outlet. Between this pressure range, a maximum in its coke profile is observed

near the top one-fifth of the catalyst bed. Similar changes in the C_5 naphthene profile with pressure are observed. Additionally, the pressure at which coke is deposited affects the TPO spectra. An increase in the total pressure of the Pt catalyst produces a TPO spectrum similar to that of Pt–Re. Furthermore, the gas-phase composition influences the distribution of coke on the surface of the catalysts.

When Pt and Pt–Re catalysts are being operated under the same conditions, their initial dehydrocyclization activities at their corresponding outlets are the same and they have the same initial C_5 naphthene profile. However, the movement of the maximum toluene production rate with time on-oil for these two catalysts is affected by their coke profiles. On the basis of this and the above observation of the effects of pressure and Re on the coke and C_5 naphthene profiles of Pt catalysts, we propose that the smaller amount of coke deposited on Pt–Re compared to Pt is due to the lower dehydrogenating capacity of the bimetallic catalyst arrived from higher hydrogen concentration on the surface of the bimetallic catalyst. This reduces coke formation on their acid sites.

The higher hydrogen concentration on the surface of the Pt–Re catalyst increases the cracking activity of the bimetallic catalyst and results in a hydrogen molar fraction below the inlet value of 0.75 throughout the catalyst bed (after 15 h time on-oil), whereas Pt shows a hydrogen molar fraction above 0.75 for the major part of the run.

ACKNOWLEDGMENT

The authors thank Dr. Gary McVicker for helpful discussions and suggestions in the preparation of this article.

REFERENCES

1. Kluksdahl, H. E., U.S. Patent 3,415,737 (1969).
2. Augustine, S. M., Alameddin, G. N., and Sachtler, W. M. H., *J. Catal.* **115,** 217 (1989).
3. Parera, J. M., Beltramini, J. N., Querini, C. A., Martinelli, E. E., Churin, E. J., Aloe, P. E., and Figoli, N. S., *J. Catal.* **99,** 39 (1986).
4. Rek, P. J. M., Dens Hrtog, A. J., and Ponec, V., *Appl. Catal.* **46,** 213 (1989).
5. P. Biloen, Helle, J. N., Verbeek, H., Dautzemberg, F. M., and Sachtler, W. M. H., *J. Catal.* **63,** 112 (1980).
6. Barbier, J., Corro, G., Zhang, Y., Bournonville, J. P., and Franck, J. P., *Appl. Catal.* **3,** 327 (1982).
7. Dees, M. J., and Ponec, V., *J. Catal.* **115,** 347 (1989).
8. Barbier, J. Churin, E., and Marecot, P., *J. Catal.* **126,** 228 (1900).
9. Carter, J. L., McVicker, G. B., Weissman, W., Kmak, W. S., And Sinfelt, J. H., *Appl. Catal.* **3,** 327 (1982).
10. McVicker, G. B., and Ziemiak, J. J., *Appl. Catal.* **14,** 229 (1985).
11. Burch, R., and Mitchell, A. J., *Appl. Catal.* **6,** 121 (1983).
12. Ostrovskii, N. M., Chalganov, E. M., Demanov, Yu. K., Kolomytsev, Yu. N., and Bogomolova, O. B., *React. Kinet. Catal. Lett.* **41**(2), 277 (1990).
13. Lietz, G., Völter, J., Dobrovolszky, M., and Paál, Z., *Appl. Catal.* **13,** 77 (1984).
14. Davis, B. H., *J. Catal.* **46,** 348 (1977).
15. Völter, J., Leitz, G., Ukleman, M., and Hermann, M., *J. Catal.* **68,** 42 (1981).
16. Parera, J. M., Querini, C. A., Beltramini, J. N., and Figoli, N. S., *Appl. Catal.* **32,** 117 (1987).
17. Bowman, P., and Biloen, P., *J. Catal.* **48,** 209 (1977).
18. Franck, P., and Martino, G., *in* "Progress in Catalyst Deactivation" (J. L. Figueiredo, Ed.), p. 365. Nijhoff, The Hague, 1982.
19. Franck, J. P., and Martino, G. P., *in* "Deactivation and Poisoning of Catalyst" (J. Oudar and H. Wise, Eds.). Dekker, New York, 1985.
20. Margitfalvi, J., Szedlacsek, P. Hegedüs, M., and Nagy, F., *Appl. Catal.* **15,** 69 (1985).
21. Völter, J., and Kürschner, U., *Appl. Catal.* **8,** 167 (1983).
22. Wilde, M., Pönitzsch, L., Feldhaus, R., and Anders, K., *Appl. Catal.* **65,** 117 (1990).
23. Figoli, N. S., Beltramini, J. N., Martinelli, E. E., Sad, M. R., and Parera, J. M., *Appl. Catal.* **5,** 19 (1983).
24. Fung, S. C., Querini, C. A., and McCoy, C. J., *in* "Catalyst Deactivation 1991" (C. Bartholomew and J. Butt, Eds.), p. 135. Elsevier, Amsterdam/New York, 1991.
25. Acharya, D. R., Ghassemi, M. R., and Hughes, R., *Appl. Catal.* **58,** 53 (1990).
26. Delahay, G., and Duprez, D., *Appl. Catal.* **53,** 95 (1989).
27. DePaw, R. P., Froment, G. F., *Chem. Eng. Sci.* **30,** 789 (1975).
28. Levinter, M. E., Borthevich, M. I., Zabotin,

L. I., and Berkovich, L. M., *Kinet. Catal.* **16,** 181 (1975).
29. Butt, J., and Petersen, E. E., "Activation, Deactivation and Poisoning of Catalyst." Academic Press, London, 1988.
30. Froment, G. F., and Bishoff, K. B., *Chem. Eng. Sci.* **16,** 189 (1961).
31. Froment, G. F., and Bishoff, K. B., *Chem. Eng. Sci.* **17,** 105 (1962).
32. Blasco, V., Royo, C., Menendez, M., Santamaria, J., and Fierro, J. L. G., *in* "Catalyst Deactivation 1991" (C. H. Bartholomew and J. B. Butt, Eds.), p. 629. Elsevier, Amsterdam, 1991.
33. Fung, S., and Querini, C. A., *J. Catal.* **138,** 240 (1992).
34. Barbier, J., Churin, E., Marecot, P., and Menezo, J. C., *Appl. Catal.* **36,** 277 (1988).
35. Zhorov, Yu. M., Panchenkov, G. M., and Kartashev, Yu. N., *Kinet. Catal.* **21,** 580 (1980).
36. Parera, J. M., Verderone, R. J., and Querini, C. A., *in* "Catalyst Deactivation 1987" (B. Delmon and G. F. Froment, Eds.). Elsevier, Amsterdam, 1987.
37. Cooper, B. J., and Trim, D. L., *in* "Catalyst Deactivation 1980" (B. Delmon and G. F. Froment, Eds.), p. 63. Elsevier, Amsterdam, 1980.
38. Bishara, A., Stanislaus, A., and Hussain, S. S., *Appl. Catal.* **13,** 113 (1984).
39. Beltramini, J. N., Cabrol, R. A., Churin, E. J., Figoli, N. S., and Parera, J. M., *Appl. Catal.* **17,** 65 (1985).
40. Beltramini, J. N., Martinelli, E. E., Churin, E. J., Figoli, N. S., and Parera, J. M., *Appl. Catal.* **7,** 713 (1983).
41. Querini, C. A., Figoli, N. S., and Parera, J. M., *Appl. Catal.* **32,** 133 (1987).
42. Figoli, N. S., Beltramini, J. N., Martinelli, E. E., Aloe, P. E., and Parera, J. M., *Appl. Catal.* **11,** 201 (1984).
43. Bertolacini, R. J., and Pellet, R. J., *in* "Catalyst Deactivation 1980" (B. Delmon and G. F. Froment, Eds.), p. 73. Elsevier, Amsterdam, 1980.
44. Parera, J. M., Figoli, N. S., Beltramini, J. N., Churin, E. J., and Cabrol, R. A., *in* "Proceedings, 8th International Congress on Catalysis, Berlin, 1984." Dechema, Frankfurt-am-Main, 1984.
45. Iglesia, E., Baumgartner, J. E., and Meitzner, G. D., *in* "Proceedings, 10th International Congress on Catalysis, Budapest, Hungary, 1992" (L. Guczi, Ed.).
46. Iglesia, E., Baumgartner, J. E., and Price, G. L., *J. Catal.* **134,** 549 (1992).